TRIPLE WALL BALLISTIC LIMIT EQUATION

Frank Schäfer and Robin Putzar

Fraunhofer EMI (Ernst-Mach Institute), Eckerstraße 4, 79104 Freiburg, Germany,
Email: schaefer@emi.fhg.de, putzar@emi.fhg.de

ABSTRACT

This paper presents a new ballistic limit equation for the case of a triple plate structural set-up consisting of bumper shield (first wall), primary structure wall (second wall) and a rear wall representing, for example, the front casing of a component located inside the spacecraft (third wall). The idea of the developed equation is to split the penetration process into two phases: the projectile impact on the first wall which generates the "primary fragment cloud", and subsequently the encounter of the primary fragment cloud with the inner walls that constitute a Whipple shield ("inner Whipple shield"). The key aspect of the model is to define an "equivalent projectile" that has the same damage capability to the second and third wall as the primary fragment cloud. The ballistic limit of the inner Whipple shield is then calculated using an established Whipple Shield Ballistic Limit Equation (BLE). The mass of the equivalent projectile is assumed equal to the total primary fragment cloud mass multiplied with a fit function C. This function was defined and was fit against 9 different configurations for Triple Wall configurations for which test data exist from former hypervelocity impact test campaigns.

1. INTRODUCTION

Vulnerability analysis for spacecraft is presently performed by determining the probability of no penetration (PNP) of the structure wall. In the case of single bumper shielded shell structures, a suitable Whipple Shield Equation is presented (e. g. in Christiansen, 1993). The current approach assumes that the equipment placed behind the spacecraft's structure wall fails upon penetration of the structure wall. However, this approach does not consider the intrinsic protection capability of the equipment's housing, e. g. the front plate of an E-Box or the wall of a pressure vessel. Consider Fig. 1, where an Al 2219 vessel with a 1.0 mm wall thickness, water-filled and pressurized with 29.8 bar Nitrogen was placed 100 mm behind a shielded spacecraft structure (bumper shield 0.8 mm Al-alloy, spacing 96.6 mm, structure wall 3.3 mm Al-alloy). The impacting projectile (Al-sphere d=5.7 mm, v=7.0 km/s, α=30°) clearly penetrated the structure wall but caused only a tiny puncture in the pressure vessel's front wall (indicating "near BL" comnditions). Hence, reliable ballistic limit equations developed for the case of a "triple wall structural set-up" consisting of bumper shield (first wall), primary structure wall (second wall) and a rear wall representing, for example, the front of a component placed inside the spacecraft (third wall) are required to allow realistic risk analysis that considers explicitly the penetration resistance offered by the third wall of such a set-up.

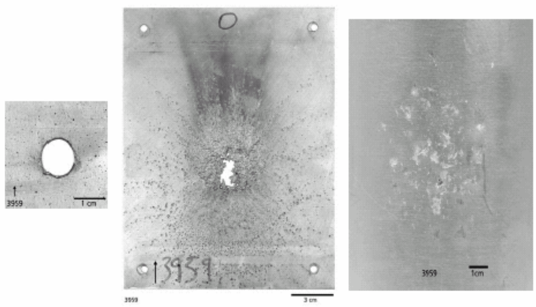

Figure 1. Exp. 3959: damages to target. EMI Exp. 3959: double-bumper shield: 0.8 mm Al, spacing 96.6 mm, 3.3 mm Al, spacing 100 mm, Al 2219 vessel, 1.0 mm wall thickness, pressure 29.8 bar (water-filled), Al-projectile d=5.7 mm, v=7.0 km/s, α=30°. From left to right: bumper plate, primary structure, vessel's front surface

2. DESCRIPTION OF THE TRIPLE WALL BALLISTIC LIMIT EQUATION

The case for which the equation was developed is shown in Fig. 2. The set-up represents a triple plate structure consisting of bumper, primary structure, and rear wall. They are indicated as first, second and third wall, respectively. The considered set-up is typical for single bumper shielded manned spacecraft structures with equipment placed behind the structure wall, or for double bumper shielded spacecraft structures, which

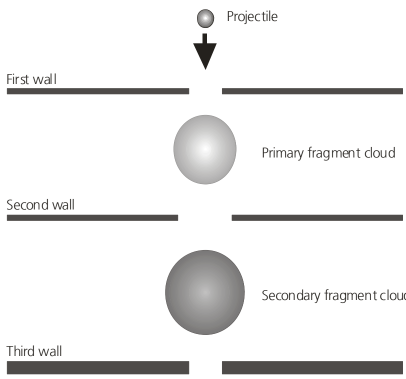

Figure 2. Triple plate structure consisting of outer bumper, inner bumper (corresponding to structure wall) and rear wall (casing wall).

Proceedings of the Fourth European Conference on Space Debris, Darmstadt, Germany, 18-20 April 2005
(ESA SP-587, August 2005)

have been investigated e. g. during the development of the Columbus Meteoroid and Debris Protection Shield (MDPS), see e. g. (Schneider, 1988).

The idea of the model is to define a projectile equivalent in terms of damage capability, to the primary fragment cloud generated from the impact of the projectile on the first wall. The impact of the projectile with the first wall creates a primary fragment cloud that eventually encounters a structure equivalent to a Whipple Shield. This “Whipple Shield” consists of the second and third wall (structure wall and casing of subsystem, respectively). For this Whipple Shield the ballistic limit diameter is calculated using the Whipple Shield Ballistic Limit Equation from Christiansen/ Cour-Palais (Christiansen, 1993).

For the presented approach, the critical particle diameter that was calculated with the above Whipple Shield Equation has to match the equivalent particle diameter that represents the primary fragment cloud (see Fig. 3). An iterative procedure described in the following computes the equivalent projectile diameter that represents the primary fragment cloud impacting on the Whipple Shield, as shown in Fig. 3.

Christiansen’s Whipple Shield Equation (Christiansen, 1993) provides the critical diameter of a particle leading to failure of the “Whipple Shield” structure wall (i.e. component casing). This critical particle diameter is compared to the equivalent particle diameter which represents the fragment cloud generated by the real particle impacting on the outer bumper. The critical projectile diameter is said to be reached, when the critical particle diameter and the equivalent particle diameter match. As such, the projectile which is initially fragmented into the ‘equivalent projectile’ fragment cloud, is defined as the ballistic limit of the whole triple plate structure. Notice that this method is iterative.

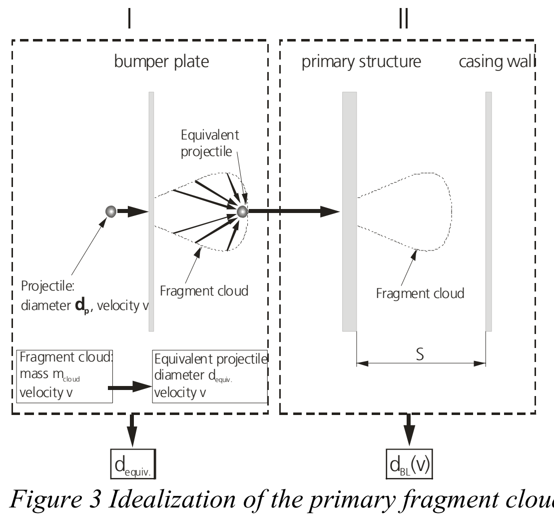

Figure 3 Idealization of the primary fragment cloud as an equivalent projectile

One important assumption for the calculations was that the velocity of the equivalent projectile was assumed to be equal to the primary fragment cloud leading edge velocity. This assumption was made because the most damaging fragments in a fragment cloud typically stem from the projectile and are mainly concentrated in the leading edge of the cloud (Piekutowski, 1996), which has approximately the same velocity as the impacting particle, if t/d_p is small.

For oblique impact, it was additionally assumed that the magnitude and direction of the equivalent projectile velocity vector is equal to the velocity vector of the projectile before the impact.

The next step was the definition of the total mass of the fragment cloud created by the impact between the projectile and the first wall. Assuming that no mass is lost due to backsplash, the fragment cloud will consist of the projectile material and the material coming from the outer bumper. In order to define the mass of the material coming from this bumper, the hole diameter must be computed for both normal and oblique impact. Knowing the outer bumper hole diameter, it is possible to calculate the primary fragment cloud mass using the equation for normal impact

$$m^{prim} = \left(m_p + m_{ob}\right) = m_p + \pi \cdot \frac{D_h^2}{4} \cdot t_{ob} \cdot \rho_{ob} \tag{1}$$

or

$$m^{prim} = m_p + \pi \cdot \frac{D_{\min} \cdot D_{\mathrm{maj}}}{4} \cdot t_{ob} \cdot \rho_{ob} \tag{2}$$

for oblique impact.

Where

m^{prim}	primary fragment cloud mass
D_h	hole diameter in the outer bumper.
D_{min}	minor axis of the elliptic hole in the outer bumper (oblique impact).
D_{maj}	major axis of the elliptic hole in the outer bumper.
t_{ob}	outer bumper thickness
ρ_{ob}	density of the outer bumper material.
m_p	projectile mass
m_{ob}	mass of the outer bumper that contributes to the primary fragment cloud.

The mass of the equivalent projectile is assumed equal to the total primary fragment cloud mass multiplied with a fit function *C.* This fit function has a value of less than 1, taking into account that only a portion of the total mass of the projectile and ejected bumper mass actually enters the space behind the second bumper.

$$m_{eqproj} = m^{prim} \cdot C \tag{3}$$

where C is assumed to be a function of the ratio of outer bumper thickness to projectile diameter, i.e.

$$C = f\left(\frac{t_{ob}}{d_p}\right) \quad (4)$$

By derivation from experimental data, see Chapter 3, the equation was fit to

$$C = 0.0022 \cdot \left(\frac{t_{ob}}{d_p}\right)^{-2} \quad (5)$$

The equivalent projectile diameter can be computed as follows:

$$d_{eqproj} = \sqrt[3]{\frac{6 \cdot m_{eqproj}}{\pi \cdot \rho_p}} \quad (6)$$

Further assumptions have been made:

- the density of the equivalent projectile is set equal to the density of the impacting projectile
- the spacing between the first and the second wall is ignored for the time being

Hole geometry for normal impact:
For normal impact, the hole diameter is calculated using an equation presented in (Baker and Persechino, 1993).

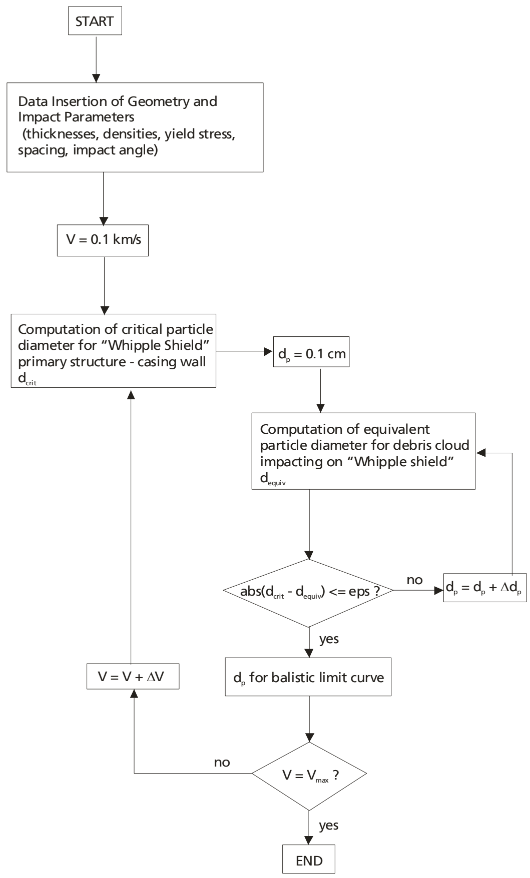

Figure 4. Flow diagram of ballistic limit curve computation for EMI Triple Wall approach

Fig. 4 shows the flow diagram of the iterative procedure. The value of the impact velocity, beginning with 0.1 m/s and gradually increased, is used to initially permit calculation of the critical diameter for the corresponding Whipple Shield. The velocity is also concurrently used in a loop that is to be computed until the exit condition (the difference between critical particle diameter for Whipple shield and equivalent particle diameter has to be smaller than the predefined value ε = 0.01 mm) is fulfilled. The outer loop increases the impact velocity until the previously defined velocity limit is reached.

3. CALIBRATION OF THE TRIPLE WALL BALLISTIC LIMIT EQUATION

The EMI Triple Wall Equation has been calibrated using impact test data on triple wall configurations (Fig. 5) from (Schneider et al., 1988; Schonberg et al., 1993; Schäfer, 2000, 2001). The total number of impact datasets used for calibration of the equation is 57. The characteristics of the triple wall structures from which the experimental data is obtained are summarized in Tab. 1. The material yield stress is provided only for the rear wall, since this is the only structural component for which the yield stress is required in the equations. The yield stresses were taken from MIL Handbook 5. The structures, their references and the number of test data that were used for calibration are listed in more detail in Tab. 1.

Figure 5. Triple wall configuration

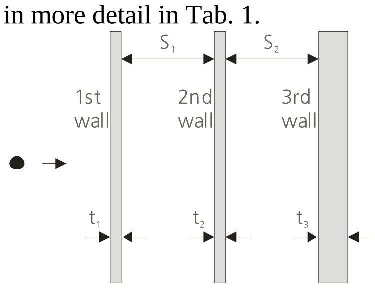

The range of impact velocities covered by the impact tests on the configurations listed in Tab. 1 was between 2 km/s and 8.5 km/s. The corresponding projectile diameters ranged from 2-10 mm, and the impact angles were 0°, 30°, 45°, 60, and 75°. All projectiles were spheres made from aluminium alloys. The range of validity of the Triple Wall Equation is thus constrained by these ranges.

The Triple Wall Equation or, more specifically, the "C" function, Equ. (5), has been fitted to the test data. To this purpose: a "best guess" function for "C" was defined; the corresponding Triple Wall Curves were determined, and; the predictions from the equation were compared with the impact test data of the configurations listed in Tab. 2. In an iterative effort, the optimum coefficients of the "C" function were fitted to yield the best Ballistic Limit Curve predictions for each dataset. In Fig. 6, the line with value "1" denotes the normalized ballistic limit curve of each configuration with failure criterion "detached spall". The circles denote test results that have been reported as "failed", the crosses denote test results that have been reported as "not failed". If test data are predicted correctly, the "failed" test cases should be located above the normalized ballistic limit curves and the "not failed" test cases should be located below the normalized ballistic limit curve. As can be seen in Fig. 8, a majority of the test results have been predicted correctly using the "C" function shown in Equ. (5). Two test datasets have been predicted slightly too optimistic and 8 test datasets have been predicted slightly conservative.

Table 1. Configurations used for calibration of the TWE (t_1 & mat'l$_1$, S_1, t_2 & mat'l$_2$, S_2, t_3 & mat'l$_3$)

Config. Ref.	Description (thickness, mat'l, spacing)	No. of tests
(Schneider, 1988)	0.8 (Al 2024 T3), 60 0.8 (Al 2024 T3), 60 3.2 (Al 2219 T851)	16
(Schneider, 1988)	0.8 (Al 2024 T3), 60 1.6 (Al 2024 T3), 60 2.4 (Al 2219 T851)	1
(Schneider, 1988)	1.6 (Al 2024 T3), 60 0.8 (Al 2024 T3), 60 2.4 (Al 2219 T851)	4
(Schneider, 1988)	0.8 (Al 6061 T6), 60 0.8 (Al 6061 T6), 60 3.2 (Al 2219 T851)	23
(Schäfer, 2000, 2001)	0.8 (Al 6061 T6), 96.6 3.3 (Al 6061 T6), 100 1.0 (Al 2219 T851)	3
(Schonberg, 1993)	0.8 (Al 6061 T6), 25.4 0.8 (Al 6061 T6), 76.2 3.175 (Al 2219 T87)	4
(Schonberg, 1993)	0.8 (Al 6061 T6), 50.8 0.8 (Al 6061 T6), 50.8 3.175 (Al 2219 T87)	4
(Schonberg, 1993)	0.8 (Al 6061 T6), 76.2 0.8 (Al 6061 T6), 25.4 3.175 (Al 2219 T87)	2

4. SUMMARY AND CONCLUSIONS

For the case of a triple wall structural set-up a ballistic limit equation was developed. The considered configurations are typical for single bumper shielded manned spacecraft structures with equipment placed behind the structure wall or for double bumper shielded spacecraft structures. The failure criterion is defined as detached spall from the third wall. 57 impact datasets were used for calibration of the equation, including impact velocities of between 2 km/s and 8.5 km/s, projectile diameters between 2 and 10 mm, and impact angles of 0°, 30°, 45°, 60, and 75°.

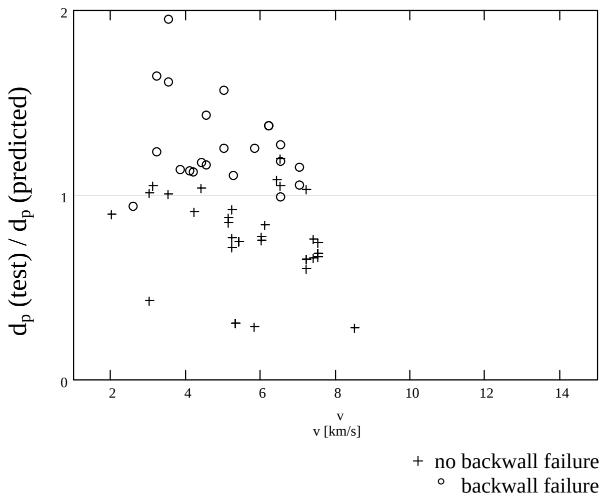

Figure 6. Normalized Ballistic Limit Curve plot of the test configurations reported in Tab. 2 plotted versus the actual impact test datasets of the corresponding test data from Tab. 2.

5. REFERENCES

Baker J. R., Persechino M. A., An Analytical Model of Hole Size in Finite Plates for Both Normal and Oblique Hypervelocity Impact for all Target Thicknesses Up To The Ballistic Limit, Int. J. Impact Engineering Vol.14, 1993

Christiansen E., Design and Performance Equations for Advanced Meteoroid and Debris Shields, *International Journal of Impact Engineering*, Vol.14, pp.145-156, 1993

Piekutowski A. J., Formation and Description of Debris Clouds Produced by Hypervelocity Impact, *NASA Contractor Report 4707*, Contract NAS8-38856, MSFC, February 1996

Schäfer F., Geyer T., “ATV MDPS for PVM/AVM, Investigatory Study, Final Report”, EMI No. E-59/99, March 16, 2000

Schäfer F., Hypervelocity Impact Testing. Impacts on Pressure Vessels, *Final Report to ESA Contract No. 10556/93/NL/PP(SC)*, EMI No. I-27/01, Ernst-Mach-Institut, Freiburg, Germany, April 30, 2001

Schneider E., Stilp A., Kleinschnitger K., Weber K., Columbus Meteroid/Debris Protection Shield (MDPS). Phase II Impact Study Final Report, EMI, 1988

Schonberg W. P., Peck J. A., Multi-Wall Structural Response to Hypervelocity Impact: Numerical Predictions vs Experimental Results, Int. J. Impact Engineering Vol. 13, No. 1, 1993